Asian Journal of Engineering and Applied Technology
ISSN 2249-068X Vol. 1 No. 2, 2012, pp.26-30

Stability of Journal Bearings Considering Slip Condition: A Non Linear Transient Analysis

Raghunandana[1*], John[2] and Kanthraj[3]

[1]*Department of Mechatronics Engineering, Manipal Institute of Technology, Manipal, Kranataka, India*
[2,3]*Department of Mechanical Engineering, Manipal Institute of Technology, Manipal, Karnataka, India*
[*] *Corresponding author E-mail:raghu.bhat@manipal.edu*

Abstract **- The no-slip boundary condition is the foundation of traditional lubrication theory. For most practical applications the no-slip boundary condition is a good model for predicting fluid behavior. However, recent experimental research has found that for special engineered surfaces the no-slip boundary condition is not applicable. In the present study the non linear transient analysis of an engineered slip/no-slip surface on journal bearing performance is examined. Numerical Analysis is carried out by solving the modified Reynolds equation satisfying the boundary conditions using successive over relaxation scheme in a finite difference grid which gives the steady state pressure. An attempt is made to evaluate the mass parameter (a measure of stability) besides finding out the steady-state characteristics of the finite journal bearing.**

Keywords**: Journal Bearings, No slip, Non Linear Transient Analysis, Mass Parameter**

I. Introduction

The basic principle of fluid film lubrication in the Reynolds' equation is that there is no slip of the liquid lubricant against the two, bounding, and solid surfaces. This 'no-slip' boundary condition assumption enables the velocity gradient within the fluid film to be determined and hence the Reynolds continuity equation is to be derived. Engineered slip/no-slip surfaces can be obtained by modification of their roughness and their surface energy. In a closely related area, researchers are trying to use the properties of engineered slip/no-slip surfaces to improve the tribological performance of lubricated contacts. Such surfaces can be obtained by modification of their roughness and their surface energy. In practise, geometric patterns can be burned on such surfaces using photolithographic processes or machining. It is then necessary to make these surfaces hydrophobic by grafting or deposition of hydrophobic compounds. They can also be obtained by dispersion of micrometric particles in a gel or a resin applied to the surface. In this case, particles are inherently hydrophobic. Such surfaces can also be made hydrophobic by depositing nanofibres, i.e. fibre of nanometre size, on these surfaces, followed up by a chemical reaction on these nanofibres.

The hydrodynamic behaviour of lubricated contacts is largely governed by the boundary conditions of the fluid flow that provides lubrication. In conventional contacts, the hydrodynamic behaviour is fully determined by the Reynolds equation, even in the presence of cavitation, if it satisfies the condition of Navier. Recent studies have shown that under certain conditions of specially treated surfaces – the Navier condition is no longer verified. Indeed, fluid slippage might occur at the solid boundary [1]. Surfaces with this feature are called non-wettable or hydrophobic.

In 1999, Watanabe et al. [2] published their experimental study of flow through a pipe with highly water repellant walls. The pipe measured 16 mm in diameter and had a highly water repellent coating applied to it. They also found that the slip velocity, extrapolated from measurements of the macroscopic flow field, was directly proportional to the shear stress.

In 2001, Zhu and Granick [3] published their experimental research on rate dependant slip for molecularly smooth surfaces. In this study a drop of Newtonian liquid was placed between two partially wetting smooth surfaces whose spacing was vibrated. The hydrodynamic forces were measured and compared to those predicted by the no-slip boundary condition. They found good agreement with the no-slip condition at low speeds. Above a critical level, however, the results deviated from the prediction. Hydrodynamic forces for higher speeds became up to 2–4 orders of magnitude less than expected by assuming the no-slip boundary condition, implying partial slip.

From the numerical point of view, it can be described by two models: the so-called slip length model and the limiting shear stress model [4]. The slip length model states that the slip velocity is proportional to the liquid shear rate evaluated at the interface. When the shear rate is low, the slip length model can describe the slip behavior. The limiting shear stress model assumed that there is a limiting shear stress at the solid–liquid interface. Using this model, Wu *et al.* [5] gave a numerical analysis for liquid slip at a solid surface and showed a good agreement with the existing experimental investigations.

Spikes analyzed the potential application of the slip surfaces on hydrodynamic lubrication [6, 7]. The bearing used in the analysis was a plane pad slider bearing with a homogeneous slip surface. The focus of the analysis was the effect of critical shear stress on load support and frictional losses as well as the feasibility of slip surfaces in low load contacts. The numerical analyses of Salant and Fortier [8, 9], using the modified slip length model [1], revealed that a heterogeneous slip/ no-slip surface in both the slider bearing and the journal bearing gives rise to a reduction of friction and an increase of load support.

In the present study, the exploitation of the slip phenomenon to investigate the stability performance of journal bearings is examined by means of a numerical analysis. By constructing an engineered heterogeneous bearing surface, on which slip occurs in certain region and is absent in others, the flow pattern in the liquid lubricating film can be altered. It is believed that a judicious choice of a pattern of slip/no-slip regions will lead to improved bearing characteristics.

II. Analysis

The journal bearing configuration is as shown in Fig. 1. The shaft and the sleeve have a clearance denoted as *c*. The operational eccentricity of the shaft and the sleeve, as measured along the line of centers, is denoted by *e*. The thickness of the lubricant film is a function of the bearing clearance, eccentricity and circumferential location and is given as

$$h(\theta) = c + e\cos(\theta) \quad (1)$$

The θ axis originates and ends at the line of centers where the film thickness is a maximum. Minimum film thickness occurs at θ equal to π.

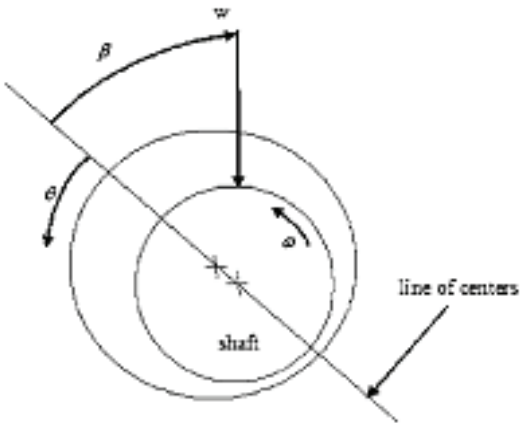

Fig. 1 Journal Bearing Configuration

Fig. 2a) illustrates the film thickness distribution. Surface 1 corresponds to the surface of the shaft and is moving at a speed *wR* Surface 2 is the stationary surface and represents the bearing sleeve. The slip/no-slip is applied on surface 2 and is as shown in Fig. 2 b). Region I is the region on which slip is imposed, while region II is the no-slip region. The slip velocity in region I is proportional to the surface shear stress, resulting in the boundary conditions.

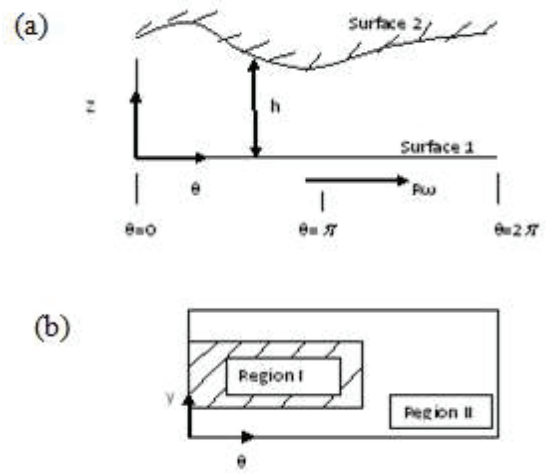

Fig. 2 (a) Film Thickness Distribution

(b) Slip/No-Slip Pattern

At z = 0 $u_\theta = u_s$, $u_y = 0$,

At z = h $u_\theta = -\alpha\mu\frac{\partial u_\theta}{\partial z}$, $u_y = -\alpha\mu\frac{\partial u_y}{\partial z}$,

Where α is the slip coefficient.

With the basic assumptions, we have the Navier-Stokes equation in the form

$$\frac{\partial^2 u_x}{\partial z^2} = \frac{1}{\mu}\frac{\partial p}{\partial x} \quad (2) \qquad \frac{\partial^2 u_z}{\partial z^2} = \frac{1}{\mu}\frac{\partial p}{\partial y} \quad (3)$$

Integrating these equations twice and applying the boundary conditions we have the velocity components

$$u_x = \frac{z^2}{2\mu}\frac{\partial p}{\partial x} - \frac{hz}{2\mu}\frac{\partial p}{\partial x}\left(\frac{h+2\alpha\mu}{\alpha\mu+h}\right) - \left(\frac{u_s z}{\alpha\mu+h}\right) + u_s \quad (4)$$

$$u_y = \frac{z^2}{2\mu}\frac{\partial p}{\partial y} - \frac{h}{2\mu}\frac{\partial p}{\partial y}\left(\frac{h+2\alpha\mu}{\alpha\mu+h}\right)z \quad (5)$$

On the basis of continuity of flow and assuming no supply of lubricant in the z direction for the journal bearing we have

$$\frac{\partial q_x}{\partial x} + \frac{\partial q_y}{\partial y} = 0 \quad (6)$$

Where $q_x = \int_0^h u_x\,dz$ and $q_y = \int_0^h u_y\,dz$ (7)

Integrating u_x and u_y under the limits and substituting these flow values in the continuity equation we have the modified Reynolds equation for a liquid lubricant film in the journal bearing, taking account of the slip as:

$$\frac{1}{R^2}\frac{\partial}{\partial\theta}\left[\frac{h^3}{12\mu}\frac{\partial p}{\partial\theta}\left(1+\frac{3\alpha\mu}{h+\alpha\mu}\right)\right] + \frac{\partial}{\partial y}\left[\frac{h^3}{12\mu}\frac{\partial p}{\partial y}\left(1+\frac{3\alpha\mu}{h+\alpha\mu}\right)\right] = \frac{\partial}{\partial\theta}\left[\frac{\omega h}{2}\left(1+\frac{\alpha\mu}{h+\alpha\mu}\right)\right] + \frac{\partial h}{\partial t} \quad (8)$$

In the dimensionless form it is represented as:

$$\frac{\partial}{\partial\theta}\left\{H^3\frac{\partial\bar{p}}{\partial\theta}\left(1+\frac{3A}{(H+A)}\right)\right\}+\left(\frac{D}{L}\right)^2\frac{\partial}{\partial Y}\left\{H^3\frac{\partial\bar{p}}{\partial Y}\left(1+\frac{3A}{(H+A)}\right)\right\}=6\frac{\partial}{\partial\theta}\left\{H\left(1+\frac{A}{H+A}\right)\right\}+12\,\Omega\frac{\partial H}{\partial T} \quad (9)$$

On substitution of A = 0 in the above equation, we arrive at the standard Reynolds equation which does not consider the slip.

III. Solution Scheme

A. Steady-State Analysis

Equation (9) is solved for the pressure using the finite difference method with SOR scheme. The pressure boundary conditions are:

1. $\bar{p}\ (\theta\ ,\bar{z})=0\ for\ \theta=\ \theta_1\ and\ \theta=\ \theta_2$
2. $\bar{p}=0\ at\ \bar{z}\ \pm 1.0$
3. $\frac{\partial\bar{p}}{\partial z}\ (\theta\ ,0)=0$
4. $\frac{\partial\bar{p}}{\partial\theta}=0\ at\ \theta=\ \theta_2$

Since the bearing is symmetrical about its central plane $(\bar{z}=0)$, only one half of the bearing needs to be considered for the analysis. Once the pressure distribution is evaluated at the steady state condition the load carrying capacity $(\overline{W})$ and the attitude angle $(\emptyset)$ are calculated.

$$\overline{W_r}=\ -\int_0^1\int_{\theta_1}^{\theta_2}\overline{p_0}\cos\theta\ d\theta\ d\bar{z} \quad (10)$$

$$\overline{W_0}=\ -\int_0^1\int_{\theta_1}^{\theta_2}\overline{p_0}\sin\theta\ d\theta\ d\bar{z} \quad (11)$$

$$\emptyset_0=\ tan^{-1}\left(\frac{\overline{W_0}}{\overline{W_r}}\right) \quad (12)$$

The steady-state load is expressed as

$$\overline{W_0}=\sqrt{\overline{W_r}^2+\overline{W_0}^2} \quad (13)$$

Sommerfeld number is evaluated as

$$S=\frac{1}{\pi\overline{W_0}} \quad (14)$$

The dimensionless friction force in the θ direction is found by integrating the shear stress over the surface area.

$$F=\int_0^{2\pi R}\int_{-L/2}^{L/2}\tau_x\ dy\ dx \quad (15)$$

Where $\tau_x=\frac{\partial u_x}{\partial z}$. Once the values of friction force and load are evaluated coefficient of friction is found from

$$f=\frac{F}{W}=\ f\left(R/c\right) \quad (16)$$

B. Stability Analysis

For stability analysis a non-linear time transient analysis is carried out using the following equations of motion.(given in non-dimensional form) for a rigid rotor supported on two identical bearing (Fig.1)

$$\bar{M}\,\overline{W_0}\left[\ddot{\varepsilon}-\varepsilon\left(\dot{\emptyset}^2\right)\right]=\overline{W_r}+\overline{W_c}\cos\emptyset \quad (17)$$

$$\bar{M}\,\overline{W_0}\left[\varepsilon\,\ddot{\emptyset}-2\,\varepsilon\left(\dot{\emptyset}\right)\right]=\overline{W_0}-\overline{W_c}\sin\emptyset \quad (18)$$

Since a unidirectional constant load is considered here, the load remains constant in direction and magnitude over the period of time and is equal to the steady-state load carrying capacity, i.e. $\overline{W_c}=\ \overline{W_0}$. The hydrodynamic forces under steady-state conditions are found for the initial condition. The equations of motion are solved by the fourth-order Runge-Kutta method to obtain $\varepsilon\ ,\emptyset\ ,\dot{\varepsilon}\ and\ \dot{\emptyset}$ for the subsequent time step by solving the partial differential equations for pressure satisfying the aforementioned boundary conditions. Now the new values of $\varepsilon\ ,\dot{\varepsilon}\ and\ \dot{\emptyset}$ are introduced in equation (9) to determine the hydrodynamic forces. These forces along with the steady-state load and mass parameter are utilized for the solution of equations (17) and (18). The process is repeated until we get a trajectory that describes the status of the system.

IV. Results And Discussion

A. Steady-State Analysis

The results got by solving the dimensionless Reynolds equation (10) are tabulated in Table 1. These results are verified with the slip coefficient value of A = 0 as calculated by Pinkus (10) which is the standard Reynolds equation. The results are in good agreement.

Table I Comparison Of Sommerfeld Number, Friction Force And Attitude Angle

	Eccentricity Ratio	Present	Pinkus(11)
Sommerfeld Number	0.2	0.6309	0.632
	0.5	0.1786	0.179
	0.8	0.0446	0.0448
Frictional Force	0.2	12.6669	12.9
	0.5	4.2343	4.31
	0.8	1.6862	1.71
Attitude Angle	0.2	74.0634	74
	0.5	56.8043	56
	0.8	36.2567	36

Figure 3 shows the pressure distribution for a bearing with a length to width ratio, L/D = 1, eccentricity ratio

ε = 0.8 for a conventional bearing and a bearing with a dimensionless slip coefficient of 10 and slip applied in region I. It is observed that the bearing with a dimensionless slip coefficient is flattened due to slip.

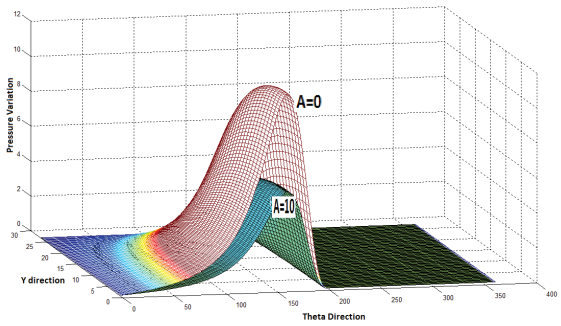

Fig. 3 Pressure distribution for L/D=1 and ϵ =0.8.

B. Stability Analysis

Initially the critical mass parameters at different eccentricity ratios are found from the trajectories of the centre of the journal. The results of the slip coefficient A = 0 using Swift-Stieber boundary conditions are verified with those of Majumdar *et. al* [11]. Since the results show very good agreement, these are not reproduced here. Some representative results are given here. One can obtain more data following the above method of solution.

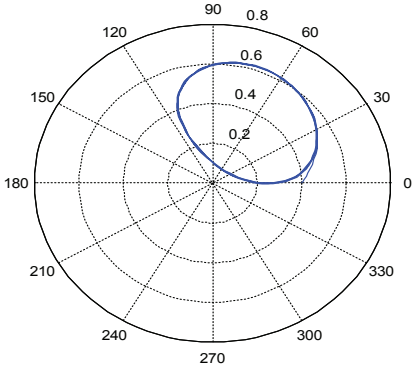

Fig. 4 Trajectory of the centre of journal under unidirec tional constant load (L/D=1.0, ϵ = 0.4, A = 0).

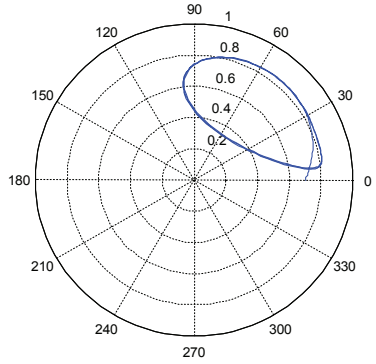

Fig. 5 Trajectory of the centre of journal under unidirectional constant load (L/D=1.0, ϵ = 0.7, A = 0).

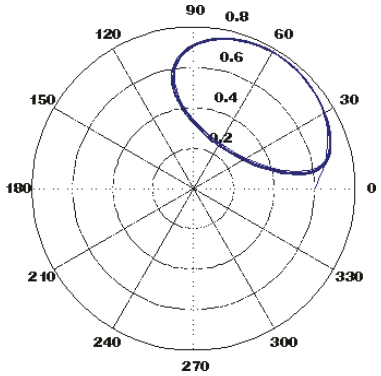

Fig. 6 Trajectory of the centre of journal under unidirectional constant load (L/D=1.0, ϵ = 0.6, A = 2).

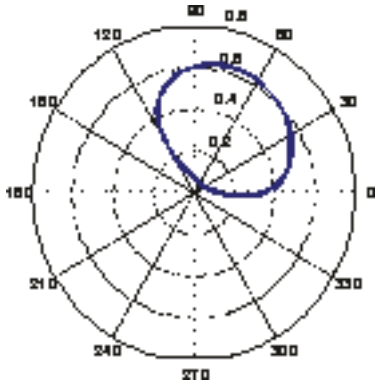

Fig. 7 Trajectory of the centre of journal under unidirectional constant load (L/D=1.0,ϵ = 0.4, A = 2).

An attempt is then made to study the effects of the slip coefficient on critical mass parameter. Critical mass parameter for a particular eccentricity ratio is found when the trajectories of journal centre ends in a limit cycle or it changes its trend from stable to unstable. Four such trajectories are shown in figures 3, 4, 5 and 6 for critical mass parameters 6, 11, 2.75 and 2.6 respectively.

Critical mass parameters can be evaluated using the same methodology for different L/D ratios and various values of slip coefficient A.

TABLE II CRITICAL MASS PARAMETERS FOR L/D = 1

Eccentricity Ratio	A = 0	A = 2
0.2	6.2	2.9
0.3	5.8	2.4
0.4	6	2.6
0.5	6.3	2.6
0.6	7.1	2.75
0.7	11	4

It is observed that the mass parameter decreases as the slip coefficient increases, which suggests that for the system to be stable when slip exists, the journal should rotate at lesser speeds.

V. Conclusions

The following conclusions are evident from the study.

1. In general the stability decreases with the increase in the slip coefficient.
2. When the slip coefficient is considered, the stability increases sharply for heavily loaded bearings ($\epsilon > 0.6$)
3. A short bearing (L/D < 1.0) gives higher stability characteristics.

Nomenclature

A Dimensionless slip coefficient, $(\alpha \mu / C)$

C Clearance (m)

D Bearing Diameter (m)

Eccentricity (mm), e , $\varepsilon \quad \varepsilon = e/C$ $(Dimensionless)$

$\bar{F}$ Dimensionless Friction Force $(FC^2/\mu \omega R^3 L)$

$\bar{f}$ Dimensionless friction coefficient

H Dimensionless film thickness, (h/C)

h Minimum film thickness (m)

M Mass of rotor (kg)

$\bar{M}$ Dimensionless mass parameter $(MC\omega^2/W_0)$

p Pressure (Pa)

$\bar{p}$ Dimensionless pressure, $(p C^2/\mu \omega R^2)$

S Sommerfeld Number

u_s Shaft surface speed, ωR

u_x Component of velocity in x direction (m/s)

u_y Component of velocity in y direction (m/s)

Steady-state load,

W_0 , $\overline{W_0}$ $\overline{W_0} = \frac{W_o C^2}{\mu \omega R^3 L}$ (Dimensionless)

W_c , $\overline{W_c}$ $\overline{W_c} = \frac{W_c C^2}{\mu \omega R^3 L}$ Unidirectional constant load,

(Dimensionless)

x, z coordinates

τ_x Dimensionless shear stress in circumferential direction. (Pa – s)

α Slip coefficient $(m^3/N\,s)$

$\emptyset$ Attitude angle

θ Circumferential coordinate

μ Viscosity, Pa-s.

ω Angular speed. (rad/s)

Acknowledgements

The author wishes to thank Manipal University for the support of the research.

References

[1] Vinogradova OI. 'Slippage of water over hydrophobic surfaces. *International Journal of Mineral Processing*' 1999; 56(1–4):31–60.

[2] Watanabe K, Udagawa Y, Udagawa H. 'Drag reduction of Newtonian fluid in a circular pipe with a highly water-repellent wall.' *Journal of Fluid Mechanics* 1999; 381:225–38.

[3] Zhu Y, Granick S. 'Limits of the hydrodynamics no-slip boundary condition'. *Physical Review Letters* 2002; 88(10):1061021–4.

[4] Bair S, Winer WO. 'High pressure high shear stress rheology of liquid lubricants.' *Journal of Tribology*1992; 114(1):1–13.

[5] Ma GJ, Wu CW, Zhou P. 'Wall slip and hydrodynamics of two-dimensional journal bearing.' *Tribology International* 2007; 40 (7): 1056 – 66.

[6] Spikes HA. 'The half-wetted bearing. Part 1: extended Reynolds equation.' Proceedings of the Institution of Mechanical Engineers, Part J: *Journal of Engineering Tribology* 2003; 217(1): 1–14.

[7] Spikes HA. 'The half-wetted bearing. Part 2: potential application in low load contacts.' Proceedings of the Institution of Mechanical Engineers, Part J: *Journal of Engineering Tribology* 2003; 217(1):15–26.

[8] Fortier AE, Salant RF. 'Numerical analysis of a journal bearing with a heterogeneous slip/no-slip surface.' *Journal of Tribology* 2005; 127(4):820–5.

[9] Salant RF, Fortier AE. 'Numerical analysis of a slider bearing with a heterogeneous slip/no-slip surface.' *Tribology Transactions* 2004; 47(3):328–34.

[10] Oscar Pinkus & Beno Sternlicht (1961), "*Theory of Hydrodynamic lubrication*", McGraw-Hill Book Company.

[11] Majumdar BC, Brewe DE "*Stability of a rigid rotor supported on oil-film journal bearings under dynamic load*." NASA Technical Report 87 – C – 26, 1987, pp.1 – 10.